

1 Retinograd-AI: An Open-source 2 Automated Fundus Autofluorescence 3 Retinal Image Gradability Assessment 4 for Inherited Retinal Dystrophies

5
6 Gunjan Naik^{*,1,2,3}, Saoud Al-Khuzaei^{*,4,5}, Ismail Moghul^{*,1,2,3}, Thales A. C. de Guimaraes^{1,2,3},
7 Sagnik Sen⁴, Malena Daich Varela^{1,2,3}, Yichen Liu¹, Pallavi Bagga^{1,2,3}, Dun Jack Fu^{1,2,3},
8 Mariya Moosajee^{1,2,3}, Savita Madhusudhan⁶, Andrew Webster^{1,2,3}, Samantha De Silva^{4,5},
9 Praveen J. Patel^{1,2,3}, Omar Mahroo^{1,2,3}, Susan M Downes^{4,5}, Michel Michaelides^{1,2,3},
10 Konstantinos Balaskas^{1,2,3}, Nikolas Pontikos^{*,1,2,3,+}, William Woof^{*,1,2,3}

11
12 ¹ University College London Institute of Ophthalmology, 11-43 Bath Street, London, UK
13 ² Moorfields Eye Hospital NHS Foundation Trust, 162 City Road, London EC1V 2PD, UK
14 ³ NIHR Biomedical Research Centre at Moorfields Eye Hospital NHS Foundation Trust and UCL
15 Institute of Ophthalmology, London, UK
16 ⁴ Oxford Eye Hospital, John Radcliffe Hospital, Oxford OX3 9DU, UK
17 ⁵ Nuffield Laboratory of Ophthalmology, Nuffield Department of Clinical Neuroscience, University of
18 Oxford, John Radcliffe Hospital, Oxford OX3 9DU, UK
19 ⁶ St Paul's Eye Unit, Liverpool University Hospitals NHS Foundation Trust, Liverpool, UK

20
21 *joint authors

22
23 +Corresponding author n.pontikos@ucl.ac.uk

24 Abstract

25 Purpose:

26 To develop an automated system for assessing the quality of Fundus Autofluorescence
27 (FAF) images in patients with inherited retinal diseases (IRD).

28 Methods:

29 We annotated a dataset of 2445 FAF images from patients with Inherited Retinal
30 Dystrophies which were assessed by three different expert graders. Graders marked images
31 as either gradable (acceptable quality) or ungradable (poor quality), following a strict grading
32 protocol. This dataset was used to train a Convolutional Neural Network (CNN) classification
33 model to predict the gradability label of FAF images.

NOTE: This preprint reports new research that has not been certified by peer review and should not be used to guide clinical practice.

34 Results:

35 Retinograd-AI achieves a performance of 91% accuracy on our held-out dataset of 133
36 images with an Area Under the Receiver Operator Characteristic (AUROC) of 0.94,
37 indicating high performance in distinguishing between gradable and ungradable images.
38 Applying Retinograd-AI to our full internal dataset, the highest proportion of gradable images
39 was found in the 30-50 years age group, where 84.3% of images were rated as gradable,
40 while the lowest was in 0-15 year olds, where only 45.2% of images were rated as gradable.
41 83.4% of images from male patients were rated as gradable, and 90.6% of images from
42 female patients. By genotype, from the 30 most common genetic diagnoses, the highest
43 proportion of gradable images was in patients with disease causing variants in *PRPH2*
44 (93.9%), while the lowest was *RDH12* (28.6%). Eye2Gene single-image gene classification
45 top-5 accuracy on images rated by Retinograd-AI was 69.2%, while top-5 accuracy on
46 images rated as ungradable was 39.0%. Retinograd-AI is open-sourced, and the source
47 code and network weights are available under an MIT licence on GitHub at
48 <https://github.com/Eye2Gene/retinograd-ai>

49 Conclusions:

50 Retinograd-AI is the first open-source AI model for automated retinal image quality
51 assessment of FAF images in IRDs. Automated gradability assessment through Retinograd
52 AI enables large scale analysis of retinal images, which is an essential part of developing
53 good analysis pipelines, and real-time quality assessment, which is essential for deployment
54 of AI algorithms, such as Eye2Gene, into clinical settings. Due to the diverse nature of IRD
55 pathologies, Retinograd-AI may also be applicable to FAF imaging for other conditions,
56 either in its current form or through transfer learning and fine-tuning.
57

58 Introduction

59

60 Inherited Retinal Dystrophies (IRDs) are genetically determined disorders of the retina,
61 which collectively represent a leading cause of blindness in children and the working-age
62 population. IRDs encompass a wide range of conditions with 280 different associated genes
63 identified so far (Georgiou et al., 2024; Lee et al., 2023; Pontikos et al., 2020). Retinal
64 imaging, using various imaging modalities, allows accurate phenotyping, which is important
65 in the diagnosis and follow-up of IRDs.

66

67 Fundus autofluorescence (FAF) imaging is particularly important in this regard since it can
68 yield data relating to the outer retina and retinal pigment epithelium (RPE). For instance, an
69 increased autofluorescent signal (hyper autofluorescence) can result from the accumulation
70 of autofluorescent material, such as lipofuscin, or from the loss of either photoreceptor outer
71 segments or macular luteal pigment, which usually absorbs the incoming short wavelengths
72 (Daich Varela et al., 2021). Similarly, loss of autofluorescence can be associated with the
73 loss of RPE. Particular patterns of autofluorescence are associated with certain IRDs, such
74 as the hyper autofluorescent flecks that are usually associated with Stargardt disease (Pichi
75 et al., 2018).

76

77 The quality of imaging data is a critical factor for developing AI models and in particular
78 during selection of scans for training AI models such as Eye2Gene and AIRDetect (Nguyen
79 et al., 2023; Pontikos et al., 2022; Woof et al., 2024). Image quality significantly influences
80 model performance and uncertainty metrics in image classification or segmentation. Poor
81 quality images frequently cause AI model failures, whereas clinicians would disregard these
82 as ungradable or request repeat imaging.

83

84 Image gradeability refers to if an image is sufficient for a human (or AI) specialist to make an
85 informed decision on the basis of the image. Although gradability is technically distinct from
86 image quality, these aspects are highly correlated and in the literature the terms are often
87 used interchangeably (Huynh et al., 2024). Manually grading images is laborious and
88 subjective, which highlights the need for automated gradability assessment to filter out poor-
89 quality imaging data. This is crucial for selecting images for training AI models and for using
90 these models to assess biomarkers in clinical trials. These approaches are also necessary
91 for deployment of AI systems in the real world setting by employing automated grading as a
92 pre-filtering step to assess whether repeat imaging is necessary and prevent propagation of
93 decisions based on unreliable data.

94

95 Several AI models for retinal image quality assessment of colour fundus images have been
96 developed (Abdel-Hamid, 2021; Abramovich et al., 2023; Chan et al., 2021; Shi et al., 2022;
97 J. Tang et al., 2022), as well as a few for assessing the quality of Spectral domain OCT (SD-
98 OCT) images (Z. Tang et al., 2024; Wang et al., 2019). However, no models currently exist
99 for other modalities such as fundus autofluorescence (FAF), and none have been specifically
100 developed for the gradability of IRDs.

101

102 Assessment of gradability of retinal scans from IRD patients poses unique challenges due
103 IRDs having a range of phenotypes depending on the gene involved. For example, large
104 areas of abnormal retina can often obstruct features such as the retinal vasculature, or
105 decreased autofluorescence can render regions darker than usual. Distinguishing these
106 pathological features from other imaging artefacts is challenging, but is crucial for reliable
107 grading and the proper functioning of AI models. Hence, in addition to their application to
108 IRDs, IRD datasets may be a good starting point for developing more general gradability
109 assessment models, as they encompass a wide range of different conditions and
110 pathologies, and affect patients across all age ranges.

111

112 We present Retinograd-AI, the first retinal image gradability assessment tool for FAF
113 imaging and the first specifically developed for all types of IRDs. Retinograd-AI is a deep
114 neural network (DNN) based classifier trained and validated on over 2400 FAF images from
115 patients seen at Moorfields Eye Hospital (MEH), annotated by three expert graders.

116

117 Methods

118 Dataset

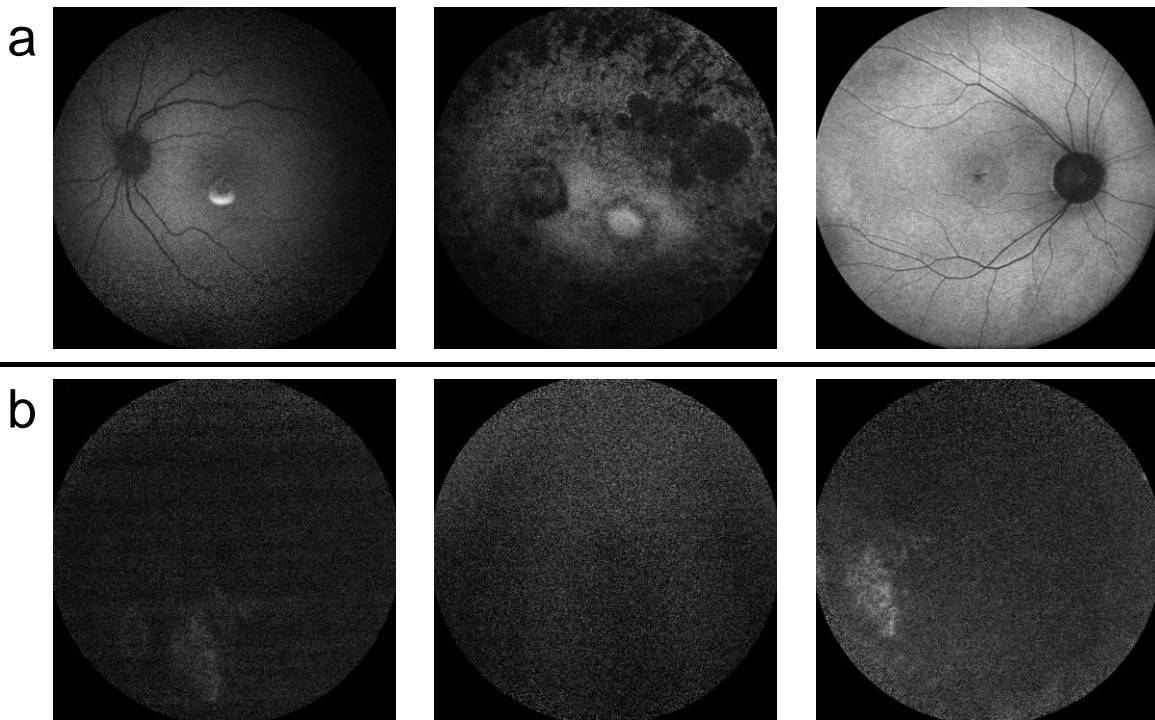
119 Our training dataset was drawn from a dataset of a total of 136,631 FAF images from 4,554
120 IRD patients from Moorfields Eye Hospital (MEH), captured using the Heidelberg Spectralis
121 imaging platform. From this dataset, 2445 images were selected at random and then
122 labelled by a team of three graders (G1, G2, G3), with 815 images assigned to each grader.
123 All graders were research fellows with over 5 years' experience in medical retina, and had
124 extensive experience with grading FAF scans for IRDs. Annotation was performed using two
125 defined criteria for image quality, as outlined in **Table 1**. This annotation was done over the
126 course of three weeks using an instance of the Label Studio tool (Tkachenko et al., 2020-
127 2022), which was hosted on our online grading platform (grading.readingcentre.org).

128

129 **Table 1:** Definition of the quality assessment criteria.

| Assessment | Criteria | Feature Visibility |
|-------------------------------------------------------------------|----------------------------------------------------------|--------------------------------------------------------------------------------------------------------------------------------------------------------------------------------------------------------------------------------------|
| Gradable (acceptable quality to a grader) | Image is sufficient to yield a grade with >50% certainty | Discrimination of the optic disc is clear and vascular arcades are visible in over $\frac{3}{4}$ of their extent. No opacities/shadowing impairing clear visibility of critical structures like the foveal and peri-foveal areas. |
| Ungradable (un-acceptable quality to a grader) | Image is not sufficient to yield a grade. | One or more anatomical features impossible to discern. |

130
131



132
133 **Figure 1:** Example images annotated as a.) gradable (acceptable quality), and b.)
134 ungradable (poor quality)
135

136 An additional 133 images were selected as a held-out test set, ensuring no patient overlap
137 with the training set, each of which were annotated by all three graders. This was used to
138 measure intergrader agreement and evaluate our algorithm. In cases where not all graders
139 agreed on the same label for a given image, the most common label was used for the
140 purposes of model evaluation. This approach helped ensure consistency and reliability in the
141 evaluation process.

142 Model Development

143

144 For training and evaluation of our Retinograd-AI model, we divided the data into training and
145 pre-test sets in a stratified way, ensuring a similar proportion of each class in both sets by
146 assigning patients to each split to avoid any overlap.

147

148 We employed an Inception Resnet v2 network architecture with imagenet pretrained weights
149 for the network. The model was trained using the Adam optimizer and cross-entropy loss,
150 with class reweighting applied to account for dataset imbalance between the two classes.
151 Horizontal flipping and random rotations to increase variability of data in line with standard
152 data augmentation practices. We have trained the model for 20 epochs, taking the best
153 performing weights determined by the validation loss as evaluated on the pre-test data. A full
154 list of hyper-parameter settings is given in **Supplementary Table 1**.

155 Results

156 The average intergrader agreement was 0.69 as measured by Cohen's Kappa (McHugh,
157 2012). A full breakdown of inter-grader agreement is given in **Supplementary Table 2**.

158

159 We evaluated Retinograd-AI on the held-out test set and compared its predictions to the
160 grader labels, viewing the problem as a binary classification task with 'gradable' being the
161 positive class and 'ungradable' being the negative class.

162

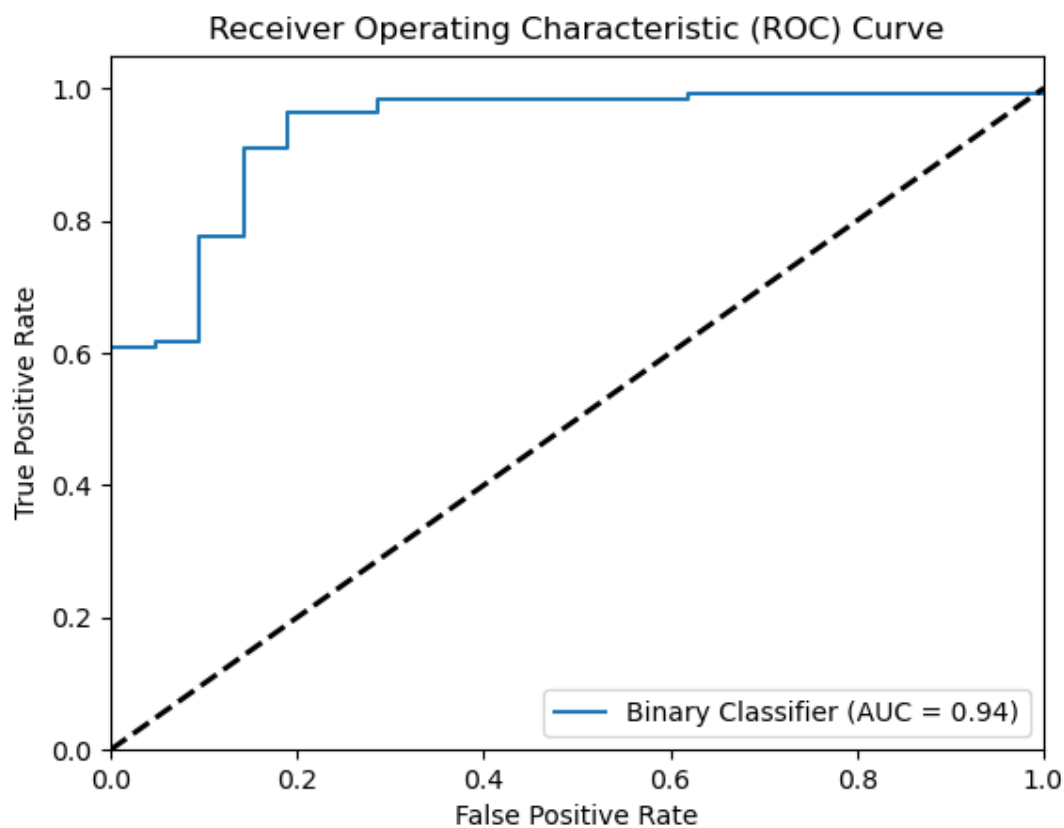
163 The model achieved an accuracy of 91% (CI₉₅=85.7-95.5%) on the held-out test set, with
164 precision of 0.96 (0.923-0.991) and recall of 0.93 (0.873-0.973). The corresponding
165 confusion matrix is given in **Table 2**. The Area Under the Receiver-Operator Characteristic
166 (AUROC) was 0.94 (**Figure 2**). Model-grader agreement (Cohen-Kappa) was 0.69, which
167 was the same as the inter-grader agreement.

168

169 **Table 2:** Model confusion matrix. Comparison of model predictions with ground-truth grader
170 labels.

| | | Model Prediction | |
|--------------|------------|------------------|------------|
| | | Gradable | Ungradable |
| Grader Label | Gradable | 104 | 8 |
| | Ungradable | 4 | 17 |

171



172

173 **Figure 2:** Receiver operator characteristic curve for the model predictions on the held-out
174 test set.

175

176 To understand how demographics might affect image quality, we applied Retinograd-AI to
177 our full dataset of 136,631 FAF images, collected as part of the Eye2Gene study, to obtain
178 Retinograd-AI predictions for each image. This enabled us to examine the relationship
179 between image quality and various other data attributes such as patient age and sex, and
180 Eye2Gene classification accuracy.

181

182

Table 3: Comparison of patient age with gradability

| Age range | % Gradable |
|-----------|------------|
| 0-15 | 45.2% |
| 15-30 | 70.5% |
| 30-50 | 84.3% |
| 50-70 | 82.7% |
| 70+ | 80.7% |

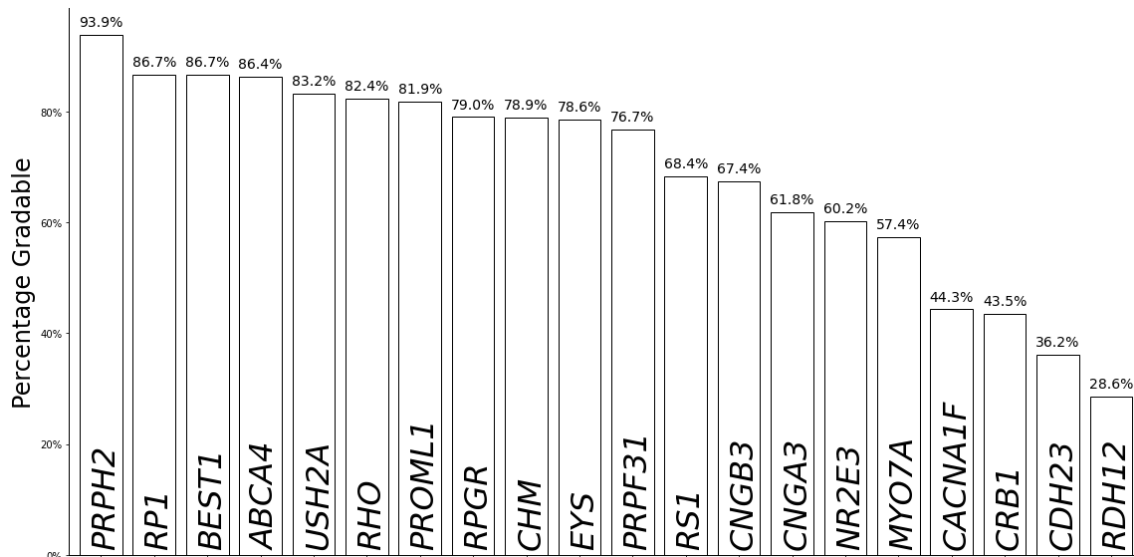
183

184 We observed a mild effect of age on Retinograd-AI assessed image quality, with the highest
185 proportions of gradable images in the 30-50 year old patients, with slightly higher proportion
186 of ungradable images in older patients, and significantly higher proportions in younger
187 patients, particularly in the under-15s (**Table 3**), which matched expectations. There was
188 also a large difference between male and female patients with images being rated as
189 gradable 83.4% of the time for male patients, and 90.6% for female patients. This difference
190 may be due to the inclusion of X-linked IRDs (*XLRP*, *CHM*) in the dataset, which affects
191 males more severely than carrier females, leading to more advanced retinal changes and
192 overall poorer image quality in males. There was also substantial variation in image quality
193 across different patient genotypes, with the highest proportion of gradable images were
194 found in patients with a disease-causing variant in *PRPH2*, with 93.9% of images were rated
195 as gradable, and the lowest being *RDH12* where only 28.6% of images were rated as
196 gradable (**Figure 3**).

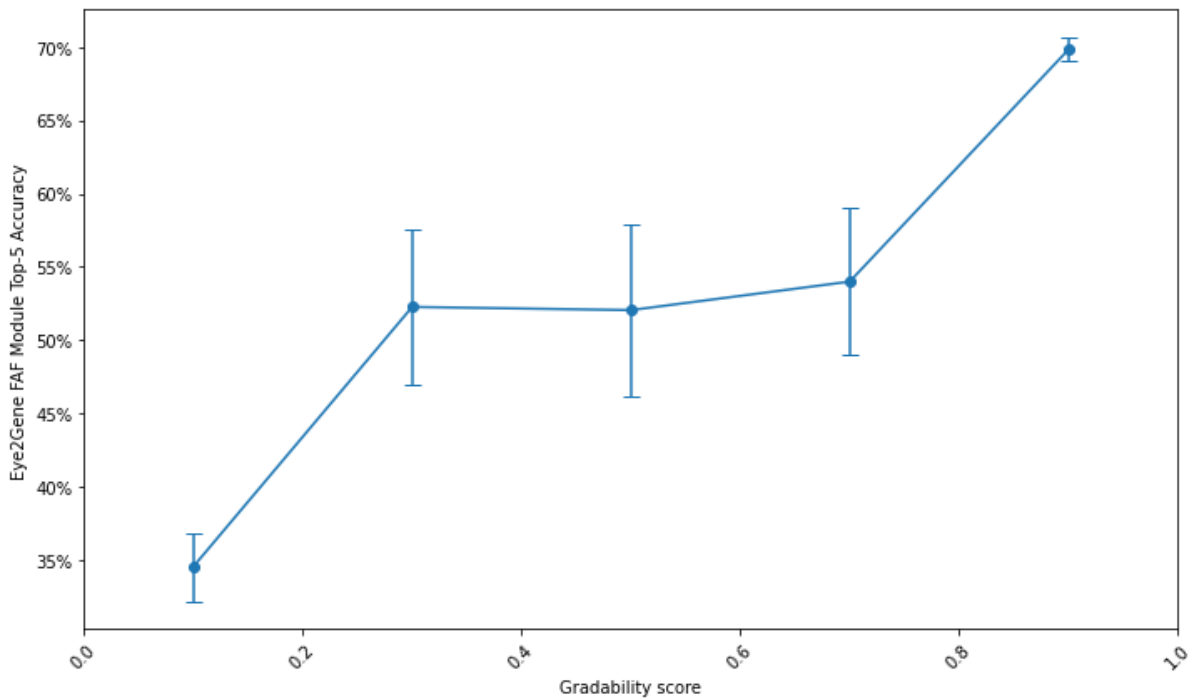
197

198 To assess how image quality affects the performance of AI models, we compared the
199 Retinograd-AI assessed image gradeability to the gene-classification accuracy of a single
200 FAF module of Eye2Gene (Nguyen et al., 2023; Pontikos et al., 2022), evaluating at image-
201 level rather than patient-level. We found that images classified as gradable by Retinograd-AI
202 had a top-5 gene classification accuracy of 69.2%, while images classified as ungradable
203 had a substantially lower accuracy of 39.0%. **Figure 4** shows how gene-classification
204 accuracy compares with the raw probability output of Retinograd, showing that higher
205 gradeability score corresponds with higher gene-classification accuracy.

206



207
208 **Figure 3:** Percentage of images rated as gradable by Retinograd-AI across the 30 most
209 common genetic diagnoses. Significant differences can be seen between genes.
210



211
212 **Figure 4:** Comparison of Eye2Gene FAF module top-5 gene classification accuracy
213 compared with gradability probability (gradability score) from Retinograd-AI. All images were
214 ranked by the probability output of Retinograd and divided into 5 buckets. For each bucket
215 the per-bucket Eye2Gene classification accuracy, and standard error, were calculated and
216 plotted.
217

218 Discussion

219

220 Herein, we present Retinograd-AI, the first retinal image quality assessment model for FAF
221 imaging and the first image quality assessment tool developed specifically for IRDs. We
222 have open-sourced our algorithm to make it available to other researchers at
223 <https://github.com/Eye2Gene/retinograd-ai> .

224

225 Retinograd-AI enabled us to automatically annotate our entire database of FAF images in
226 IRDs from Moorfields Eye Hospital, an otherwise unfeasible task to perform manually. These
227 data enabled us to gain valuable insights into image quality variability in relation to
228 parameters such as patient age, sex and genotype, which historically have been difficult to
229 separate out due to previously-unquantified influences.

230

231 As might be expected, we found that younger (0-15 year olds) and older (70+ year olds) age
232 groups had a smaller proportion of gradable images than other age groups. For IRD
233 genotypes, we found that genotypes which are earlier onset, affect the posterior pole such
234 as *RDH12* or cause widespread degeneration such as *CRB1* had a lower proportion of
235 gradable images. As did genotypes that tend to present with secondary cataract, severe
236 phenotypes or high myopia such as *MYO7A*, *NR2E3* and *CACNA1F*. Achromatopsia
237 genotypes such as *CNGB3* and *CNGBA3* often have nystagmus and photoaversion which
238 could also explain a lower proportion of gradable images in those genotypes.

239

240 We were also able to confirm our hypothesis that image quality of FAF imaging has a
241 significant impact on the performance of AI models such as Eye2Gene. This has significant
242 implications for the deployment of AI models into clinical settings.

243

244 Changes in the data quality between validation and real-world settings could have a large
245 impact on model performance, leading to substantially lower real-world accuracy than
246 expected, carrying implications for safety and efficacy.

247

248 Automated image quality assessment tools, such as Retinograd-AI, can have an important
249 role to play in addressing this, both by identifying variations in image quality between
250 different settings and patient populations, as well as for pre-screening images at point of use
251 to reject poor-quality images.

252

253 Retinograd-AI can also be used in other scenarios where image quality is important, but
254 expert feedback is not immediately available, for example, in collecting data for clinical trials.

255 In these cases Retinograd-AI can provide near real-time feedback to the operator about the
256 quality of the captured images and whether it is sufficient for downstream analysis, or
257 whether repeat imaging is recommended.

258
259 Given the diversity in age and phenotypes of IRDs, Retinograd-AI is a robust starting point
260 for building gradeability models for FAF imaging for other conditions where FAF is commonly
261 used such as Geographic Atrophy and Central Serous Chorioretinopathy, potentially via
262 transfer learning using Retinograd-AI weights as a starting point.

263
264 We expect automatic gradability annotations to prove invaluable to future image
265 classification and segmentation tasks as imaging quality is a significant confounder for many
266 image-derived metrics.

267
268 In the future, we aim to improve Retinograd-AI by incorporating additional data from other
269 conditions, as well as extend our approach to further imaging modalities.

270

271 Ethics

272 This research was approved by the IRB and the UK Health Research Authority Research
273 Ethics Committee (REC) reference (22/WA/0049) “Eye2Gene: accelerating the diagnosis of
274 inherited retinal diseases” Integrated Research Application System (IRAS) (project ID:
275 242050). All research adhered to the tenets of the Declaration of Helsinki.

276

277 Code availability

278 The source code for the Retinograd-AI model architecture training and inference is available
279 from <https://github.com/Eye2Gene/retinograd-ai> .

280

281 Data availability

282 The data that support the findings of this study are divided into two groups, published data
283 and restricted data. Published data are available from the Github repository. Restricted data
284 are curated for under a UCL Business owned license and cannot be published, to protect
285 patient privacy and intellectual property. Synthetic data derived from the test data has been
286 made available at <https://github.com/Eye2Gene/retinograd-ai>

287

288 Author contributions

289 WAW, GN, SAK and IM analysed the data and wrote the manuscript. WAW and NP
290 designed the experiments, analysed data and wrote the manuscript. NP obtained funding.
291 SS, TACG, MDV and SAK analysed the data. All authors have critically reviewed the
292 manuscript.
293

294 Acknowledgement

295
296 This work is primarily funded by a NIHR AI Award (AI_AWARD02488) which supported NP,
297 WAW, MM, KB, SD and SM. The research was also supported by a grant from the National
298 Institute for Health Research (NIHR) Biomedical Research Centre (BRC) at Moorfields Eye
299 Hospital NHS Foundation Trust and UCL Institute of Ophthalmology. NP was also previously
300 funded by Moorfields Eye Charity Career Development Award (R190031A). OAM is
301 supported by the Wellcome Trust (206619/Z/17/Z). SA is supported by a scholarship from
302 Qatar National Research Fund (GSRA6-1-0329-19010). This project was also supported by a
303 generous donation by Stephen and Elizabeth Archer in memory of Marion Woods. The
304 hardware used for analysis was supported by the BRC Challenge Fund (BRC3_027). We
305 also gratefully acknowledge the support of NVIDIA Corporation with the donation of the Titan
306 Xp GPU used for this research. The views expressed are those of the authors and not the
307 funding organisations.
308

309 References

310

311 Abdel-Hamid, L. (2021). Retinal image quality assessment using transfer learning: Spatial
312 images vs. wavelet detail subbands. *Ain Shams Engineering Journal*, 12(3), 2799–2807.
313 <https://doi.org/10.1016/j.asej.2021.02.010>

314 Abramovich, O., Pizem, H., Van Eijgen, J., Oren, I., Melamed, J., Stalmans, I., Blumenthal,
315 E. Z., & Behar, J. A. (2023). FundusQ-Net: A regression quality assessment deep
316 learning algorithm for fundus images quality grading. *Computer Methods and Programs*
317 *in Biomedicine*, 239, 107522. <https://doi.org/10.1016/j.cmpb.2023.107522>

318 Chan, E. J. J., Najjar, R. P., Tang, Z., & Milea, D. (2021). Deep Learning for Retinal Image
319 Quality Assessment of Optic Nerve Head Disorders. *Asia-Pacific Journal of*
320 *Ophthalmology (Philadelphia, Pa.)*, 10(3), 282–288.
321 <https://doi.org/10.1097/APO.0000000000000404>

322 Daich Varela, M., Esener, B., Hashem, S. A., Cabral de Guimaraes, T. A., Georgiou, M., &
323 Michaelides, M. (2021). Structural evaluation in inherited retinal diseases. *The British*
324 *Journal of Ophthalmology*, 105(12), 1623–1631. [https://doi.org/10.1136/bjophthalmol-](https://doi.org/10.1136/bjophthalmol-2021-319228)
325 [2021-319228](https://doi.org/10.1136/bjophthalmol-2021-319228)

326 Georgiou, M., Robson, A. G., Fujinami, K., de Guimarões, T. A. C., Fujinami-Yokokawa, Y.,
327 Daich Varela, M., Pontikos, N., Kalitzeos, A., Mahroo, O. A., Webster, A. R., &
328 Michaelides, M. (2024). Phenotyping and genotyping inherited retinal diseases:
329 Molecular genetics, clinical and imaging features, and therapeutics of macular
330 dystrophies, cone and cone-rod dystrophies, rod-cone dystrophies, Leber congenital
331 amaurosis, and cone dysfunction syndromes. *Progress in Retinal and Eye Research*,
332 100, 101244. <https://doi.org/10.1016/j.preteyeres.2024.101244>

333 Huynh, J., Chuter, B., Walker, E., Gonzalez, R., Bowd, C., Jalili, J., Christopher, M.,
334 Weinreb, R. N., & Zangwill, L. (2024). Distinguishing image quality from gradeability: the
335 relationship between quality and gradeability for color fundus photographs in glaucoma
336 detection. *Investigative Ophthalmology & Visual Science*, 65(9), PB00115–PB00115.

- 337 <https://iovs.arvojournals.org/article.aspx?articleid=2800573>
- 338 Lee, K. E., Pulido, J. S., da Palma, M. M., Procopio, R., Hufnagel, R. B., & Reynolds, M.
339 (2023). A Comprehensive Report of Intrinsically Disordered Regions in Inherited Retinal
340 Diseases. *Genes*, 14(8). <https://doi.org/10.3390/genes14081601>
- 341 McHugh, M. L. (2012). Interrater reliability: the kappa statistic. *Biochemia Medica: Casopis*
342 *Hrvatskoga Drustva Medicinskih Biokemicara / HDMB*, 22(3), 276–282.
343 <https://www.ncbi.nlm.nih.gov/pubmed/23092060>
- 344 Nguyen, Q., Woof, W., Kabiri, N., Sen, S., Daich Varela, M., Cabral De Guimaraes, T. A.,
345 Shah, M., Sumodhee, D., Moghul, I., Al-Khuzaei, S., Liu, Y., Hollyhead, C., Taylor, B.,
346 Lobo, L., Veal, C., Archer, S., Furman, J., Arno, G., Gomes, M., ... Eye2Gene Patient
347 Advisory Group. (2023). Can artificial intelligence accelerate the diagnosis of inherited
348 retinal diseases? Protocol for a data-only retrospective cohort study (Eye2Gene). *BMJ*
349 *Open*, 13(3), e071043. <https://doi.org/10.1136/bmjopen-2022-071043>
- 350 Pichi, F., Abboud, E. B., Ghazi, N. G., & Khan, A. O. (2018). Fundus autofluorescence
351 imaging in hereditary retinal diseases. *Acta Ophthalmologica*, 96(5), e549–e561.
352 <https://doi.org/10.1111/aos.13602>
- 353 Pontikos, N., Arno, G., Jurkute, N., Schiff, E., Ba-Abbad, R., Malka, S., Gimenez, A.,
354 Georgiou, M., Wright, G., Armengol, M., Knight, H., Katz, M., Moosajee, M., Yu-Wai-
355 Man, P., Moore, A. T., Michaelides, M., Webster, A. R., & Mahroo, O. A. (2020). Genetic
356 Basis of Inherited Retinal Disease in a Molecularly Characterized Cohort of More Than
357 3000 Families from the United Kingdom. *Ophthalmology*, 127(10), 1384–1394.
358 <https://doi.org/10.1016/j.ophtha.2020.04.008>
- 359 Pontikos, N., Woof, W., Vaturi, A., Javanmardi, B., Ibarra-Arellano, M., Hustinx, A., Moghul,
360 I., Liu, Y., Heß, K., Georgiou, M., Pfau, M., Shah, M., Yu, J., Al-Khuzaei, S., Wagner, S.,
361 Varela, M. D., de Guimarães, T. C., Sen, S., Kabiri, N., ... Michaelides, M. (2022).
362 Eye2Gene: prediction of causal inherited retinal disease gene from multimodal imaging
363 using deep-learning. In *Research Square*. <https://doi.org/10.21203/rs.3.rs-2110140/v1>
- 364 Shi, C., Lee, J., Wang, G., Dou, X., Yuan, F., & Zee, B. (2022). Assessment of image quality

365 on color fundus retinal images using the automatic retinal image analysis. *Scientific*
366 *Reports*, 12(1), 10455. <https://doi.org/10.1038/s41598-022-13919-2>

367 Tang, J., Yuan, M., Tian, K., Wang, Y., Wang, D., Yang, J., Yang, Z., He, X., Luo, Y., Li, Y.,
368 Xu, J., Li, X., Ding, D., Ren, Y., Chen, Y., Sadda, S. R., & Yu, W. (2022). An Artificial-
369 Intelligence-Based Automated Grading and Lesions Segmentation System for Myopic
370 Maculopathy Based on Color Fundus Photographs. *Translational Vision Science &*
371 *Technology*, 11(6), 16. <https://doi.org/10.1167/tvst.11.6.16>

372 Tang, Z., Wang, X., Ran, A. R., Yang, D., Ling, A., Yam, J. C., Zhang, X., Szeto, S. K. H.,
373 Chan, J., Wong, C. Y. K., Hui, V. W. K., Chan, C. K. M., Wong, T. Y., Cheng, C.-Y.,
374 Sabanayagam, C., Tham, Y. C., Liew, G., Anantharaman, G., Raman, R., ... Cheung,
375 C. Y. (2024). Deep learning-based image quality assessment for optical coherence
376 tomography macular scans: a multicentre study. *The British Journal of Ophthalmology*,
377 bjo – 2023–323871. <https://doi.org/10.1136/bjo-2023-323871>

378 Tkachenko, M., Malyuk, M., Holmanyuk, A., & Liubimov, N. (2020-2022). *Label Studio: Data*
379 *labeling software*. <https://github.com/heartexlabs/label-studio>

380 Wang, J., Deng, G., Li, W., Chen, Y., Gao, F., Liu, H., He, Y., & Shi, G. (2019). Deep
381 learning for quality assessment of retinal OCT images. *Biomedical Optics Express*,
382 10(12), 6057–6072. <https://doi.org/10.1364/BOE.10.006057>

383 Woof, W., de Guimarães, T. A. C., Al-Khuzaei, S., Varela, M. D., Sen, S., Bagga, P.,
384 Mendes, B., Shah, M., Burke, P., Parry, D., Lin, S., Naik, G., Ghoshal, B., Liefers, B.,
385 Fu, D. J., Georgiou, M., Nguyen, Q., da Silva, A. S., Liu, Y., ... Pontikos, N. (2024).
386 Quantification of Fundus Autofluorescence Features in a Molecularly Characterized
387 Cohort of More Than 3000 Inherited Retinal Disease Patients from the United Kingdom.
388 *medRxiv : The Preprint Server for Health Sciences*.
389 <https://doi.org/10.1101/2024.03.24.24304809>

390

391 **Supplementary**

392

393 **Supplementary Table 1:** List of hyperparameter settings used for training the neural
394 network.

| Parameter | Value |
|---------------|-------------------------------------------------------|
| Architecture | inception_resnet_v2 |
| Batch size | 4 |
| Image size | (768,768) |
| Train Epochs | 20 (Early stopping as no validation loss improvement) |
| Optimiser | Adam |
| Loss | Weighted categorical cross-entropy |
| Learning rate | 1e-5 |
| Augmentations | Horizontal flipping, Random rotations |

395

396

397 **Supplementary Table 2:** Inter-grader confusion matrix G1/2/3=Grader 1/2/3, G=Gradable,
398 U=Ungradable

| Grader 1 vs Grader 2 | | G2 | | Grader 1 vs Grader 3 | | G3 | | Grader 2 vs Grader 3 | | G3 | |
|----------------------|---|-----|----|----------------------|---|-----|----|----------------------|---|-----|----|
| | | G | U | | | G | U | | | G | U |
| G1 | G | 110 | 7 | G1 | G | 113 | 4 | G2 | G | 110 | 5 |
| | U | 5 | 11 | | U | 2 | 14 | | U | 5 | 13 |

399

400